



ISSN 1110-0451



(E S N S A)

Dynamic Performance Evaluation of N-channel MOSFET under Gamma Irradiation

A. Sharaf, Sh. M. Eladl, K. A. Sharshar and A. Nasr

Radiation Engineering Department, NCRRT, Egyptian Atomic Energy Authority, Cairo, Egypt.

ARTICLE INFO

Article history:

Received: 12th Dec. 2023

Accepted: 17th Mar. 2024

Available online: 1st Apr. 2024

Keywords:

Ionizing Radiation,
MOSFET, Switching
Characteristics,
Rise and Fall times,
Mobile Charges,
Transconductance,
Capacitance,
Threshold Voltage.

ABSTRACT

In this manuscript, the experimental studies for two groups, 2N7000 and BS107, of N-channel MOSFET are conducted. Each group, which have two devices from the same type, is exposed to dosages of gamma-ray ionizing radiation. The main objective of this study is to discuss the dynamic performance of these types under low dose ionizing radiation for purpose of usage as a low dose radiation dosimeter. Novelty of this study arisen from that the dynamic parameters such as threshold voltage, rise and fall times, the transconductance and capacitance between different device terminals are investigated. Because of gamma-ray irradiation, the surface and interface charges are arisen into MOSFET region. The threshold voltage is dependent on the MOSFET parameters, as it depends reversely on the oxide capacitance. From the obtained results, the channel width and length play an important role for determining all the dynamic parameters. One can notice that the majority of capacitances values are decreased. Consequently, the threshold voltage is decreased with the increase of radiation dose. From outcomes, the different transconductance values have different compartment according to the channel width and length into these adjacent regions. Generally, it tends to degrade with increasing the gamma-ray irradiation dose. The rise time tends to decrease while fall time tends to increase semi-linearly with increasing dosage values. From digital processing point of view, small shift in the rise or fall time will affect the pulse decision and then the information processing. Finally, one can conclude that n-channel MOSFETs under study not only have a specified response to gamma-ray radiation but also, they give a deterministic performance over the range of dose in this study. Therefore, the n-channel MOSFET under study - for both type number and dose- is a candidate to be a low dose dosimeter for gamma-ray radiation. The obtained dynamic response will be very important for any recent space or ionizing radiation environment and applications.

I. INTRODUCTION

Over the last few decades, there is a great interest in semiconductor materials as they are essential elements and they have become most important material for the fabrication of electronic and optoelectronic devices. The invention of transistors has resulted in the development of present-day society with advanced information systems [1].

Firstly, the static performance of metal-oxide semiconductor field-effect transistors (MOSFETs) was processed in previous work as in Farroh, et al. [2]. However, here another phase that is the dynamic characteristics for different two families of (MOSFETs) is studied under low dose gamma-ray radiation. It returns to

the important of completing other phases such as determination the dynamic performance for any semiconductor-based device under ionizing radiation environments.

The novelty of this work appeared explicitly in multi points that covered and given in the MOSFETs model description and, their contribution into results and discussion sections. These points include the threshold voltage, rise and fall times of N-MOSFETs devices, transconductance, and capacitance between each region and other neighbored regions. Moreover, instantaneous effects of different Gamma-ray radiations for two-group family of N-MOSFETs are studied. The novelty of this

study not only for considering the previous dynamic MOSFETs parameters, but also the investigations of commercial devices which may pave the way to indicate the behavior of standard N-MOSFET devices under the same investigation conditions.

It is not claimed that we have superiority of all outcomes but certainly, we paved the way to give other investigations that agree or enhance what have been obtained.

Electronic devices based on MOS and CMOS technologies found a great application within the high-level ionizing radiation environments like radiation therapy and radiology systems, space, accelerators and nuclear power plants. It was found that the total ionizing dose (TID) makes a shift in the threshold voltage, transconductance variation and increase the leakage current of these devices [3-5].

Electronic systems on the board of space crafts are exposed to permanent radiation from the cosmic or solar sources. These radiations may cause failures of such electronic devices and components [6-8]. The field of study of radiation induced defects in semiconductors would be very useful in evaluating the lifetime of devices experienced to radiation environment in the space applications, atomic energy installations etc. The Metal-oxide semiconductor (MOS) devices are more sensitive to radiation, even after a low dose [9-13]. In MOSFETs, the gate oxide structures play the major role in changing the electrical characteristics due to irradiation [14-16].

The $I-V$ characteristic ($I_{DS} - V_{GS}$) of the MOSFETs is degraded due to ionizing radiation [17-19]. This degradation results from electron-hole creation in the oxide layer of the transistor [20-22]. All electrical parameters concerning the transistor will be affected by this degradation. The holes are gradually deflected toward the side of Si-SiO₂ interface and get trapped there due to their lower mobility than electrons. The channel current of the MOSFET is changed and the threshold voltage is shifted due to the built up of positive charges [23 - 27]. This will make the channel current to be very sensitive to the positive charges, because they are very close to the channel. Thus, the threshold voltage shift can be exploited as a measure of the absorbed dose within the oxide layer.

Converting the threshold voltage shift (ΔV_{Th}) to the absorbed dose is a main function of the MOSFET dosimeters. These two quantities are related by [28]:

$$\Delta V_{Th} = V_{Th} - V_{Th0} = AD^n \quad (1)$$

Where V_{Th0} and V_{Th} are the threshold voltages before and after gamma irradiation, respectively, A is a constant, D is the absorbed dose and n is the degree of linearity. The n depends on factors like the voltage applied to the gate during the irradiation, the thickness of the oxide layer and on the absorbed radiation dose [29-31]. A linear dependence ($n = 1$) is more preferable and in this case the parameter A directly refers to the MOSFET sensitivity.

All applications that use the microelectronic MOSFET components in both civilian and military installation require these components to keep their functionality in the ionizing radiation environments. Different researches have paid attention to the static characteristics of MOSFT devices under radiation effect. In this article, the effect of gamma irradiation on the dynamic characteristic parameters has been investigated, on the channel charge operation, different capacitance leads, and rise and fall times. Two MOSFET transistors are evaluated experimentally before and after exposure to gamma radiation by a dose from 0.5 to 6.5 Gy as low gamma doses [32, 33],

When MOSFET is exposed to irradiation, the charges are trapped at the oxide region between source and gate and also between gate and drain. As a result, depletion in the silicon located under these oxides is affected, source and drain resistances increase and effective pinch-off voltage decreases.

Also, when CMOS device is exposed to ionizing radiation, an increment of the trapped charges at the oxide region will take place. A high generation rate of interface states will lead to threshold voltages shifting and carrier mobility generation in MOS channel [34-36].

When the dose is low, the change in the threshold voltage (ΔV_{th}) will be small. This change results from either trapped charges and generated interface states or compensation of one polarity of the charge by a charge of the opposite polarity (to increase and decrease the V_{th}).

The rest of the article is organized as follow; the MOSFET model description is presented in section II, in section III the main results from experiments and discussions are presented. Finally, the conclusion is made up in the IV section.

II. MOSFET Model Description

Studying the MOSFET performance under the influence of ionizing radiation represents an active area of research for the past decades. In fact, MOSFET finds application in instrumentation part of any electronic system. The development of MOS technology is dominant due to large packing density, low noise and low power requirement. In MOSFET, the input capacitance and the transconductance are almost independent of gate voltage and the output capacitance is also independent of the drain voltage. This offers advantages over MESFET's and JFET's. A number of models for the radiations induced changes in n-channel MOSFET have been developed [18, 19] to account for various changes in the characteristics of the device but still these models are inadequate to explain a complete simulation model [37-39]. Because of their faster switching speeds and simple drive requirements, MOSFETs are selected for this study to determine the dynamic characteristics under low dose rate.

The MOS transistor can be modeled by various degrees of complexity. However, a consideration of the actual physical construction of the device is illustrated in Figure 1. It gives some understanding of the various components of the model. The gate to channel capacitance (C_{gc}), the gate to source capacitance (C_{gs}), and the gate to drain capacitance (C_{gd}) are assigned. Also, it is shown in the model the source to bulk capacitance (C_{sb}), the gate to bulk capacitance (C_{gb}) and the drain to bulk capacitance (C_{db}).

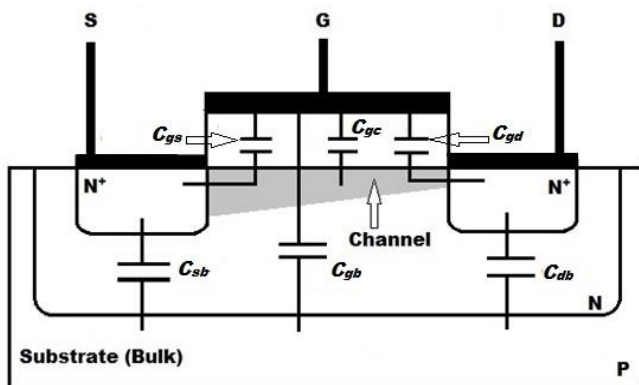


Fig (1): NMOS transistor model with capacitive mode [5].

Transconductance (G_m) is an important parameter that characterizes the MOSFET devices, and it is defined as the ratio of output current to input voltage [6];

$$G_m = \frac{\partial I_D}{\partial V_G}, \text{ at } V_D = \text{constant} \quad (2)$$

Where G_m is the transconductance, I_D is the drain current, V_G the gate voltage and V_D the drain voltage. At zero gate voltage, the transconductance is mainly the conductance of the channel G_{mo} , which can be expressed as [7]:

$$G_{mo} = q \cdot \mu_n \cdot N_D \cdot z \cdot (W_c/L_c) \quad (3)$$

Where q is the electron charge, μ_n is the electron mobility, N_D is the doping concentration, z is the channel thickness, W_c is the channel width and L_c is the channel length. As an example, and for the case of $\mu_n = 1040 \text{ cm}^2/\text{V}\cdot\text{S}$, $N_D = 6 \times 10^{15} \text{ cm}^{-3}$ and $z = 2 \times 10^{-4} \text{ cm}$, $G_{mo} = 200 (W_c/L_c)$, in which the channel width and length are an effective parameters in transconductance, as it will be seen in the results section.

From the general relation of the transconductance related to the transfer characteristics of the MOSFET devices, at the ohmic region, the G_m can be given by:

$$G_m = \mu_n C_{ox} (W_c/L_c) V_D \quad (4)$$

In which C_{ox} is the oxide capacitance per unit area. After the MOSFET transconductance is theoretically modeled, let us turn round to give some notice about the threshold voltage and its main effective parameters.

A positive charge is stored in the gate oxide under ionizing radiation and threshold voltage V_{th} shifts can be used to measure the gamma irradiation. The change in the threshold voltage ΔV_{th} depends on the gate oxide thickness. Trapped holes leave very thin oxides by tunnel effect.

In the case of low dose rate, one can notice that each of interface traps voltage; V_{it} , and threshold voltage change; ΔV_{th} , will be increased. Meanwhile, the oxide traps; V_{ot} , will be decreased. The dose charge along this portion of the track is quickly swept onto the junction by drift [7]. The threshold voltage can be stated as following:

$$V_{th} = V_{FB} + 2 \varphi_F + \frac{\sqrt{2 \epsilon_s q N_a (2 \varphi_F + V_{SB})}}{C_{ox}} \quad (5)$$

V_{th} is the threshold voltage, V_{FB} is the flat-band voltage, φ_F is a physical parameter with ($2\varphi_F$) typically 0.6 V; ϵ_s is the permittivity of silicon, N_a is the doping concentration of the p-type substrate; V_{SB} is the source to bulk voltage.

III. RESULTS AND DISCUSSIONS

At the start of this section, it is preferable to denote some hints about the main effects of the mechanism of Gamma irradiation on MOSFET devices. The oxide trapped charge and interface trapped charge will have a contribution on the threshold voltage shift. It is essentially return to the total ionizing dose (TID) which can be called cumulated ionization. The instantaneous ionization will cause single event effect (SEE). The mechanism of oxide-trapped charge in NMOS [6] will take place when the positive charge Q_{ox} is trapped in the gate oxide. As a result, the carrier density in the channel and correspondingly the current and then electric field will increase. The interface trapped charges of electron mobility will be occurred if $V_{GS} > 0$ in NMOS and vice versa in PMOS. As a result, the carrier's surface mobility will be decreased.

Rise time is the time taken for a signal to cross a specified lower voltage threshold (10% of the final value) followed by a specified upper voltage threshold (90% of the final value). Fall time is the time taken for a signal to cross a specified upper voltage threshold (90% of the initial value) followed by a specified lower voltage threshold (10% of the initial value). This is an important parameter in both digital and analog systems, which indicates how well the system preserves a fast transition in the input signal. Figure 2 shows a typical digital pulse with rise and fall time specified on the graph. The logic signals step between two values. The one value is approximately the power supply voltage while the second value is approximately the zero reference. Logic state is usually controlled by a clock signal that is a square wave. The rise and fall time of this clock signal is usually less than 10% of the clock cycle. The rise and fall times of the logic signals should be in this same range.

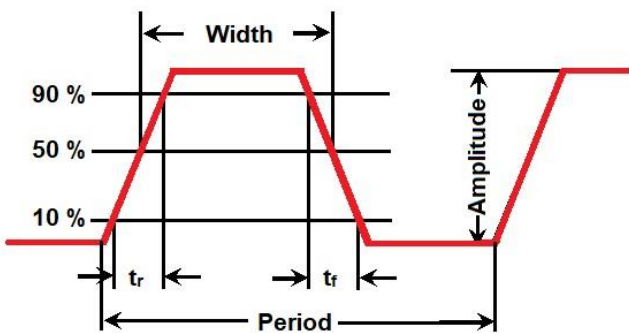


Fig. (2): Practical signal with identifications of rise and fall times

Tables 1 and 2 illustrate the change of the dynamic parameters of first group MOSFET type 2N7000 with gamma irradiation. These parameters include the capacitance leads, C_{gs} , C_{gd} , and C_{ds} , and conductance between leads, G_{gs} , G_{gd} and G_{ds} . Additionally, the output square wave rise time, t_r and the fall time, t_f are incorporated. All of these dynamic parameters are investigated before and after the exposure of the device to gamma radiation.

The applied dose range to all devices under test (DUT) is from 0.5 to 6.5 Gy. From Tables 1 and 2, it can be noticed that most of the dynamic parameters of the first group are degraded. Especially, the C_{ds} value is notably changed because of ionizing radiation. In the first group, two samples approximately have the same behavior that ensures the effect of ionizing radiation into the sample under test (SUT). Not only the rise time values will be affected by radiation but also the shape of the square wave and any further forms will be changed. From electronic point of view, it is very important to preserve the straightness, as can be possible, of the rise and fall time. This will be very important for any digital processing especially for recent multi core microprocessors.

As consequence for giving more attention to the behavior of n-channel MOSFETs, other family; second group, has type BS107 is experimentally investigated. The Tables 3 and 4 give some hints about the behavior of this type at the same condition considered before.

The general form of the transconductance depending on the various MOSFET parameters, especially the channel width and length, can be given by:

$$G_m = (\mu_n E_{in} E_o / D) (W/L) (V_{gs} - V_{th}) \quad (6)$$

A smaller ΔV_{th} results from either loss charge trapping and interface state generation or compensation of one polarity of charge by a charge of the opposite polarity (to increase and decrease the V_{th}) [8].

By investigating Tables (1 and 3), one can notice that the all capacitances values (C_{gs} , C_{gd} , and C_{ds}), rise time; t_r , and threshold voltage; V_{th} , have changed as a result of the transistor exposed to gamma-ray irradiation for all DUT, as shown in details in the following sub-sections which discuss each parameter performance.

Table (1): Illustrates the dynamic parameters of N-channel MOSFET in response to applied square wave type; 2N7000

	2N7000_Device 1					2N7000_Device 2				
	t_r (μ s)	C_{gs} (pF)	C_{gd} (pF)	C_{ds} (pF)	V_{th} (V)	t_r (μ s)	C_{gs} (pF)	C_{gd} (pF)	C_{ds} (pF)	V_{th} (V)
Pre_Irrad	2.18	15.49	25.87	16.63	1.6126	2.19	16.39	26.95	16.57	1.5888
0.50 Gy	2.17	15.07	24.53	14.57	1.5989	2.18	15.45	25.17	14.75	1.5689
1.00 Gy	2.16	14.48	24.08	13.76	1.5699	2.17	14.62	24.69	12.93	1.5541
1.50 Gy	2.15	13.63	22.71	12.31	1.5662	2.16	13.75	23.94	12.42	1.5466
2.00 Gy	2.14	12.91	22.32	11.94	1.5589	2.15	13.15	23.5	11.73	1.5313
2.50 Gy	2.13	12.66	21.71	11.53	1.5459	2.14	12.82	23.11	11.45	1.5278
3.00 Gy	2.12	12.11	21.49	10.89	1.5359	2.13	12.44	22.72	10.91	1.5174
3.50 Gy	2.11	11.98	21.35	10.36	1.5348	2.125	12.15	22.32	10.75	1.5067
4.00 Gy	2.105	11.71	21.17	10.19	1.5231	2.115	12.01	22.05	10.58	1.4972
4.50 Gy	2.1	11.48	21.02	10.07	1.5106	2.11	11.87	21.83	10.37	1.4841
5.00 Gy	2.085	11.19	20.79	9.95	1.5079	2.105	11.62	21.71	10.13	1.4608
5.50 Gy	2.065	10.97	20.51	9.87	1.4953	2.1	11.43	21.49	10.02	1.4385
6.00 Gy	2.045	10.72	20.27	9.76	1.4829	2.08	11.19	21.27	9.89	1.4147
6.50 Gy	2.028	10.55	20.04	9.51	1.4703	2.05	10.98	21.13	9.73	1.3995

Table (2): Illustrates the dynamic parameters of N-channel MOSFET in response to applied square wave type; 2N7000, (Cont.)

	2N7000_Device 1				2N7000_Device 2			
	t_f (ns)	G_{gs} (mS)	G_{gd} (mS)	G_{ds} (mS)	t_f (ns)	G_{gs} (mS)	G_{gd} (mS)	G_{ds} (mS)
Pre_Irrad	90	0.0065	0.0166	15.93	90	0.0089	0.015	16.31
0.50 Gy	150	0.0059	0.0149	14.53	140	0.0073	0.014	15.25
1.00 Gy	160	0.0046	0.0138	13.87	150	0.0065	0.013	14.79
1.50 Gy	165	0.0031	0.0123	13.35	170	0.0058	0.012	13.57
2.00 Gy	175	0.0019	0.0117	12.88	180	0.0046	0.011	13.15
2.50 Gy	180	0.0017	0.0109	12.47	185	0.0041	0.0095	12.73
3.00 Gy	183	0.0014	0.0102	12.26	185	0.0037	0.0087	12.14
3.50 Gy	185	0.0011	0.0095	11.95	190	0.0033	0.0079	11.65
4.00 Gy	187	0.0007	0.0086	11.58	193	0.0026	0.0071	11.11
4.50 Gy	192	0.0004	0.0078	11.17	197	0.0021	0.0065	10.73
5.00 Gy	196	0.0001	0.0068	10.85	201	0.0016	0.0055	10.25
5.50 Gy	199	0.00009	0.0061	10.51	205	0.0011	0.0043	9.82
6.00 Gy	201	0.00005	0.0053	10.23	208	0.0009	0.0035	9.41
6.50 Gy	205	0.00004	0.0041	9.95	211	0.0007	0.0027	9.23

Table (3): Illustrates the dynamic parameters of N-channel MOSFET in response to applied square wave type; BS107.

	BS 107_Device 1					BS 107_Device 2				
	t_r (μ s)	C_{gs} (pF)	C_{gd} (pF)	C_{ds} (pF)	V_{th} (V)	t_r (μ s)	C_{gs} (pF)	C_{gd} (pF)	C_{ds} (pF)	V_{th} (V)
Pre_Irrad	2.155	93.4	92.65	46.8	1.1695	2.185	91.75	96.87	45.35	1.1768
0.50 Gy	2.145	92.58	91.61	45.66	1.1561	2.175	90.67	94.63	41.745	1.1672
1.00 Gy	2.135	91.67	90.17	44.28	1.1474	2.165	89.58	93.51	40.16	1.1551
1.50 Gy	2.123	90.73	89.85	43.87	1.1389	2.16	88.37	92.17	39.38	1.1445
2.00 Gy	2.113	89.81	88.37	43.35	1.1289	2.155	87.25	91.45	38.71	1.1358
2.50 Gy	2.105	88.95	87.79	42.02	1.1163	2.145	86.32	90.56	37.57	1.1292
3.00 Gy	2.098	88.03	86.25	41.73	1.1124	2.138	85.17	89.25	37.2	1.1259
3.50 Gy	2.081	87.58	85.89	40.52	1.1105	2.131	84.35	88.67	36.8	1.1194
4.00 Gy	2.072	87.19	84.52	39.75	1.1087	2.128	83.95	88.11	36.35	1.1161
4.50 Gy	2.061	86.75	83.19	39.35	1.1062	2.115	83.58	87.43	35.92	1.1121
5.00 Gy	2.048	86.34	82.95	38.85	1.1047	2.103	83.41	86.97	35.48	1.1087
5.50 Gy	2.037	85.95	81.62	38.19	1.1018	2.095	83.13	86.17	35.05	1.1052
6.00 Gy	2.029	85.59	80.27	37.79	1.1003	2.069	82.91	85.57	34.68	1.1017
6.50 Gy	2.013	85.13	79.33	37.23	1.0967	2.047	82.69	84.93	34.22	1.1005

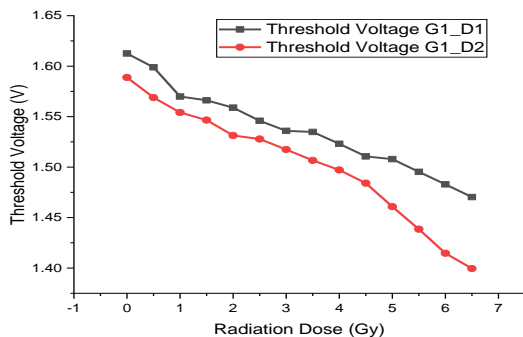
Table (4): Illustrates the dynamic parameters of N-channel MOSFET in response to applied square wave type; BS107, (Cont.)

	BS 107_Device 1				BS 107_Device 2			
	t_f (ns)	G_{gs} (mS)	G_{gd} (mS)	G_{ds} (mS)	t_f (ns)	G_{gs} (mS)	G_{gd} (mS)	G_{ds} (mS)
Pre_Irrad	75	0.0995	0.1329	0.868	70	0.0998	0.1605	0.779
0.50 Gy	150	0.0952	0.1295	0.835	130	0.0925	0.1551	0.765
1.00 Gy	155	0.0869	0.1235	0.7673	140	0.0884	0.1495	0.754
1.50 Gy	160	0.0848	0.1185	0.7587	145	0.0856	0.1458	0.737
2.00 Gy	165	0.0816	0.1125	0.7321	150	0.0834	0.1385	0.719
2.50 Gy	170	0.0752	0.1095	0.7131	157	0.0783	0.1305	0.705
3.00 Gy	173	0.0744	0.1022	0.6911	162	0.0735	0.1247	0.689
3.50 Gy	176	0.0729	0.0999	0.6751	165	0.0693	0.1215	0.651
4.00 Gy	178	0.0705	0.0978	0.6535	170	0.0672	0.1174	0.635
4.50 Gy	180	0.0692	0.0965	0.6327	175	0.0653	0.1113	0.618
5.00 Gy	185	0.0675	0.0941	0.6147	180	0.0634	0.1086	0.598
5.50 Gy	189	0.0649	0.0921	0.5987	185	0.0617	0.1018	0.573
6.00 Gy	192	0.0624	0.0875	0.5758	190	0.0602	0.0953	0.549
6.50 Gy	195	0.0605	0.0815	0.5495	192	0.0591	0.0872	0.517

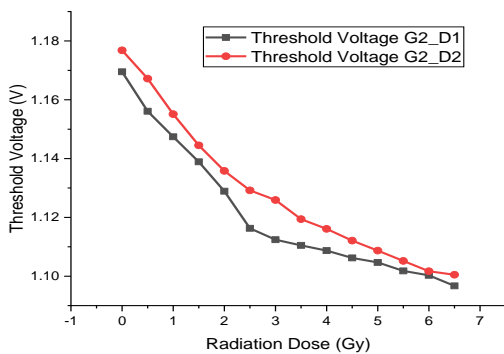
A. Threshold Voltage:

Figure 3-a illustrates the threshold voltage V_{th} with gamma doses in MOSFET type for first group (G1) (2N7000, 2 devices); as well as second group (G2) (BS107, 2 devices) is presented in figure 3-b. One can notice that the considered devices in-group one and two are normally affected by gamma radiation [17-19]. Because of the influence of different charges considered in the previous section; the oxide trapped and interface trapped charges, which will influence into threshold voltage. Meanwhile, from Figure 3, the V_{th} will degrade linearly gradually as before those two dose values.

As presented in Figure 3, the threshold voltage (V_{th}) decreases with the increase of the gamma-ray irradiation dose for n-channel MOSFET and increase with the increase of the gamma-ray irradiation dose. It is clear that the trend for all transistors in the two groups shows nearly linearly decreasing relation which indicates that the MOSFET devices can be utilized as dosimeter devices for the considered range. Although the sensitivity may be small, these because of using commercial devices. Using special types of MOSFET with large thickness of the silicon dioxide layer may tend to large device sensitivity and wide range of operations. In addition, the devices in each group confirm the same behavior at different dose rates.



(a)



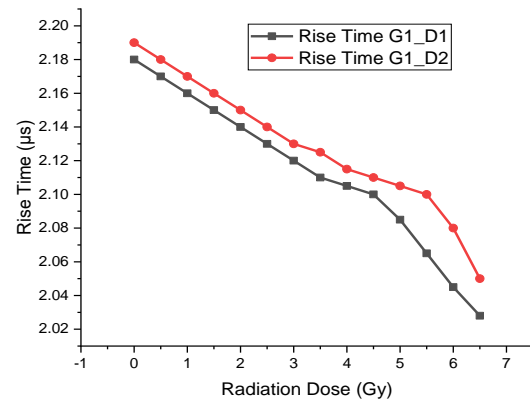
(b)

Fig. (3): Represents the n-channel MOSFET threshold voltage response to gamma-ray dose; a) first group and b) second group.

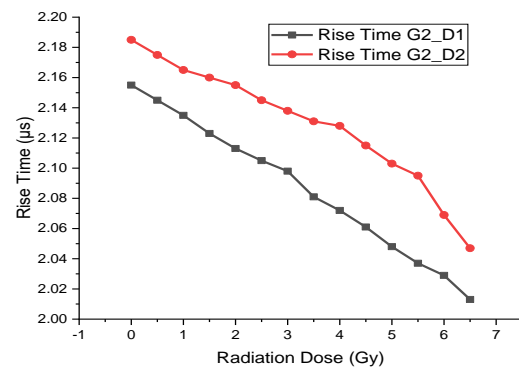
B. Rise Time:

The rise time; t_r , decreased due to the change in MOSFET capacitances between transistor leads C_{gs} , C_{gd} and C_{sd} . This decrement is alternatively at the same gamma doses applied before, as in Tables 1, 3 and Figure 4. Generally, the rise time, which is one of important dynamic MOSFET parameters, decreased by increasing of radiation doses. It could essentially due to the generation and recombination of oxide and interface traps.

From Figure 4 (a, and b), one can notice that there are minimum peaks, regardless anyone of the DUT will be less than another in each group; ($D1$ or $D2$). Because of the main target is to discuss the behavior of these devices before and after exposing to ionizing radiation. From the electronic point of view, the rise time stability is very important for change the state of logic circuits from one to zero and vice versa. Therefore, any change because of ionizing radiation should be taken into account for the sensitivity of the logic circuit, such as microprocessor final decision.



(a)

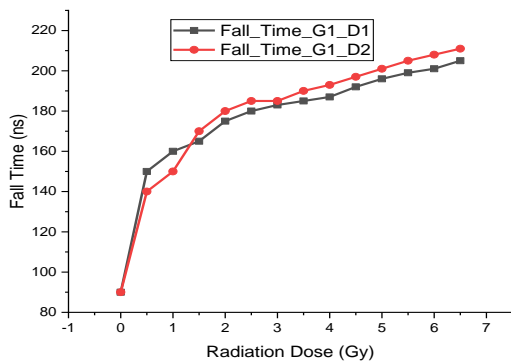


(b)

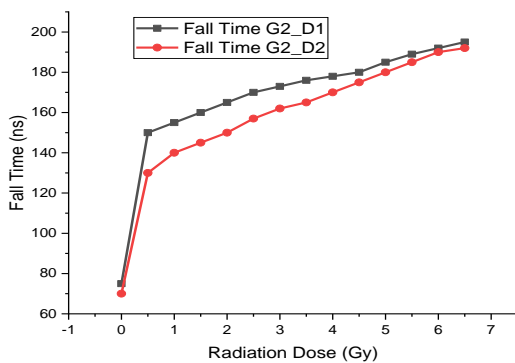
Fig. (4): Represents the n-channel MOSFET rise time in (μ s) response to gamma-ray dose; a) first group and b) second group.

C. Fall Time

Figure 5 (a, and b) indicates the response for the time and Gamma-ray doses for first group and second group respectively. One can notice that the fall time; t_f (ns), has approximately sharp linear increasing response versus the gamma-ray dose between zero and 1 Gy. After that, the fall time has a little linear increasing value for incremental dose values up to 6.5 Gy. Although the fall time increasing but this will cause disturbances in the determining the upcoming rise time for next input pulse. The effect of ionizing radiation is very critical for MOSFET application especially in space and satellite field. Let us now study the overall performance of each of rise and fall times. The first will be decreased and the second will increased due to created mobile charges in different MOSFET region. Especially, the positive oxide and negative interface trapped charges. It means that the pulse shape will be delayed and may overlap with the coming pulse period. As a result, a wrong logic gate decision may be occurred.



(a)



(b)

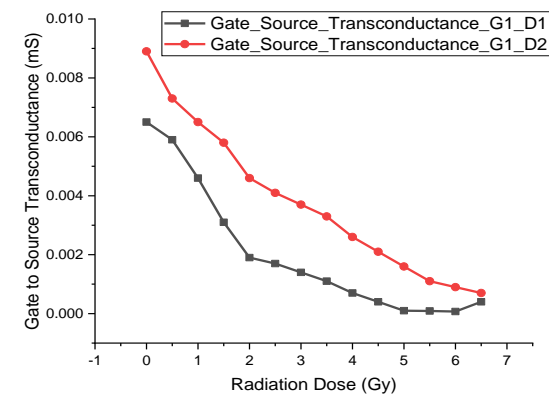
Fig. (5): Represents the n-channel MOSFET fall time in (ns) response to gamma-ray dose; a) first group and b) second group.

D. Transconductance

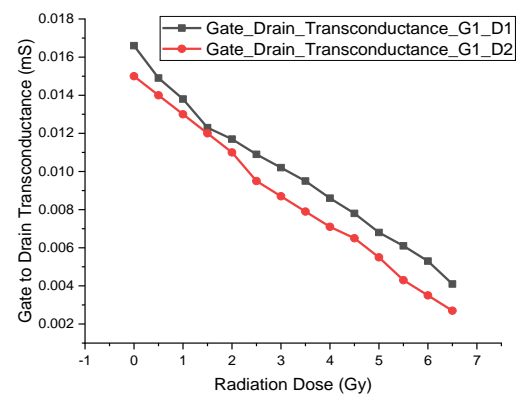
Now let us turn round to investigate different MOSFET devices transconductance (G_{gs} , G_{gd} , and G_{ds}) behavior. It denotes us the facility to distinguish between effects of them in the overall performance. Normally, the mentioned trapped mobile charges are the main reason for any changes. The value of any transconductance and after that capacitance mainly depends on the dopant concentration and then the free charges in the edges between neighbored regions. In normal operation, the transconductance value should be stable. Nevertheless, under the ionizing radiation these values may be changed. Therefore, it is important to investigate these variations and discuss the main effects into the DUT behavior.

a. Gate-Source Transconductance

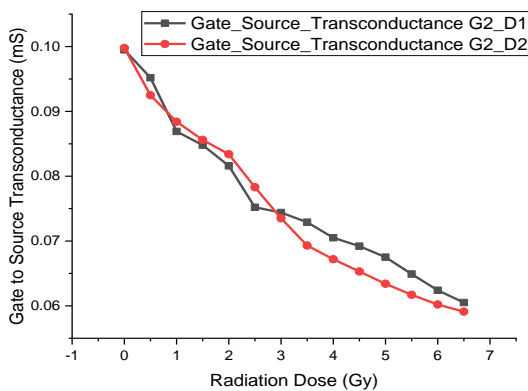
Referring to the previous description about the transconductance, especially from Equations (3-to 6), the channel width and length, and oxide silicon capacitance (W , L , and C_{ox} respectively) will play the important role for determining this G_{gs} value before and after the DUT irradiation process. Figure 6 (a, b) depicts the change of the G_{gs} as consequence of dosage values for first and second group respectively. One can notice that in Figure 6a, for first group, the G_{gs} has approximately a little decreasing liner response. Also one can notice that the value of G_{gs} is decreased after radiation averagely from 6.5×10^{-4} mS to 4×10^{-6} mS for D1 and 8.9×10^{-3} mS to 7×10^{-4} mS for D2. Meanwhile, for group 2, the G_{gs} is abruptly decreased from 0.0995 mS before radiation to 0.061 mS approximately for both devices. One can wonder about the main reason to obtain this behavior for G1 and G2. Let us discussing the coming two transconductance to give the final summery in the case of DUT.



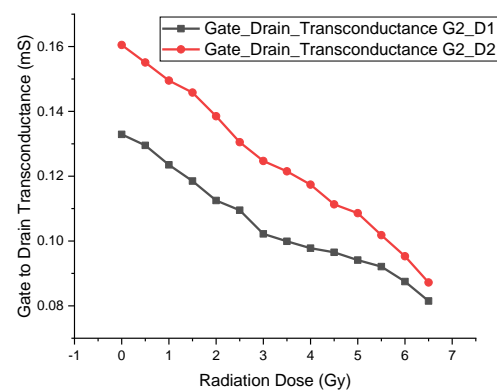
(a)



(a)



(b)



(b)

Fig. (6): Represents the n-channel MOSFET gate-source conductance response to gamma-ray dose; a) first group and b) second group.

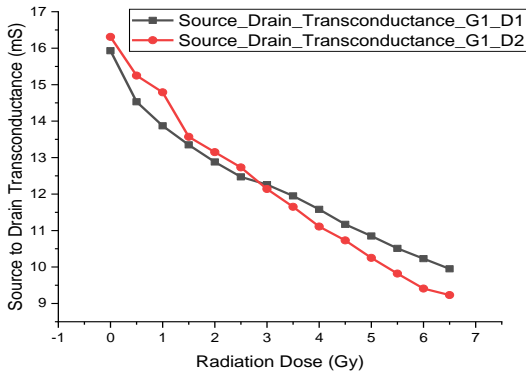
Fig. (7): Represents the n-channel MOSFET gate-drain transconductance response to gamma-ray dose; a) first group and b) second group.

b. Gate- Drain Transconductance

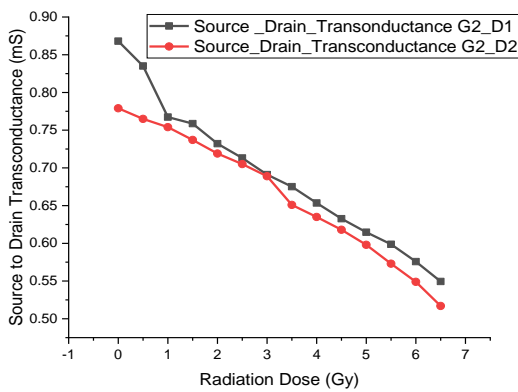
The gate to drain transconductance (G_{gd}) behavior is depicted in Figure 7 (a, and b). Once more, from the previous preface about the relation between it and MOSFET's parameters such as channel width and length, and oxide capacitance, these values depend essentially on the free carriers between gate and drain regions. From investigating Figure 7a, for G1, one can notice also that the stability of G_{gd} under the change of ionizing radiation values. It has approximately a little decreasing linear response for both groups. Nevertheless, the G_{gd} is decreased in comparison with its value before irradiation. Turn round to Figure 7b, for G2, one can impress that it denotes the same behavior in previous Figure 7a. However, the main difference is that the G_{gd} was low before ionizing radiation. From Figures 6 and 7, one can conclude that the change of G_{gs} and G_{gd} are observed because of exposing to ionizing radiation.

c. Source to Drain transconductance

Now, we will discuss the G_{sd} behavior of DUT at the same considered radiation dose. From electronic point of view, all channel width and length are taken into account. In addition, the overall oxide capacitor C_{ox} will be implied. Figure 8 depicts the G_{sd} behavior for G1 and G2 respectively. It is obviously expected that the G_{sd} will be degraded once the dosage value increased from 0.5 Gy to 0.65 Gy. The main reason returns to previous mentioned surface and interface charge which composed into the oxide region. Additionally, the silicon oxide region will directly affect the value of G_{sd} , as recognized from Equation 4, which will be confirmed from the next section, if the gate source capacitance will be decreased? In addition, one can recognize theoretically from Eq. (5, and 6) that when the oxide capacitor value decreases the threshold voltage, V_{th} , will be increased. Hereafter, the G_{sd} consequently will be decreased.



(a)



(b)

Fig. (8): Represents the n-channel MOSFET source-drain transconductance response to gamma-ray dose; a) first group and b) second group.

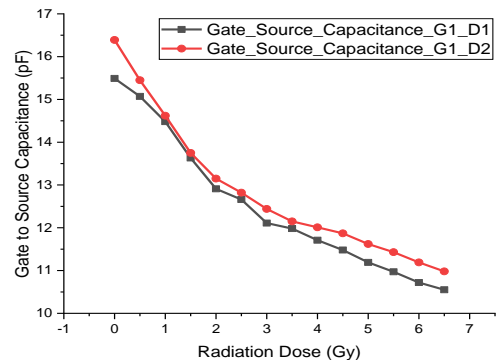
E. Capacitance Performance

a. Gate to Source Capacitance

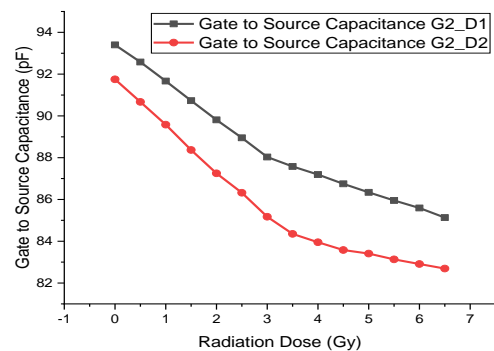
As considered before, the capacitance values will determine the transconductance and consequently the remainder of NMOSFET characterization parameters. The relation between the gate source capacitance C_{gs} and the same applied radiation dose is depicted in Tables (1, and 3) and Figure 9. One can notice that the C_{gs} is decreased with increasing the dose value radiation. It returns to generated positive charges in the N-channel of NMOSFET devices of G1 and G2. Referring to figure 9 (a and b), one can notice that the channel area between source and gate region, as in Figure 1, is larger than between drain and gate region. Therefore, the decreasing in C_{gs} is recognized in comparison with C_{gd} . The main hint when one investigates from Figure 9 (a and b) is that there is a slight increment of C_{gs} when the dose value is changed from 0.5 Gy until 6.5 Gy for G1 and G2. In the same range of the dose value, the V_{th} is decreasing as in Figure 3 (a, and b). It achieves the reverse relation between the capacitance and V_{th} as in Equation 5.

b. Gate to Drain Capacitance

From Figure 10 (a), the C_{gd} value is decreased from 27 pF, before irradiation, to about 20 pF at 6.5 Gy with continuously decreased linear response approximately in reset of doses values in the range. From Figure 10 (b), the C_{gd} values also decreased from 98 pF as initial value before irradiation to approximately 82 pF at full dose range of 6.5 Gy. Therefore, in this case, the C_{gd} is linearly decreased with increasing the doses values. The abrupt or linear change in the C_{gd} value can return to the generated positive free charges in this small channel width or area for G1 or G2 respectively. Generally, the ionizing radiation will have a lower effect in the outcomes of Figure 10 in comparison with Figure 9. As it was considered in previous section, due to the limited area of the channel between gate and drain as shown previously in Figure 1, the change in C_{gd} will be approximately small, as shown in Figure 10 (a and b). It refers essentially to the free positive charge density in this N-channel, which results from surface and interface charges. These mobile charges composed into the oxide region. Nevertheless, free carriers in that region will be lower in comparison to their numbers between source and gate region.

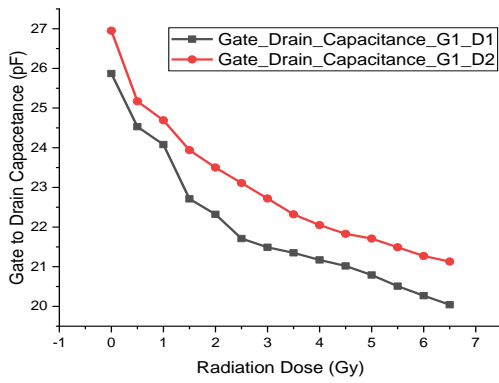


(a)

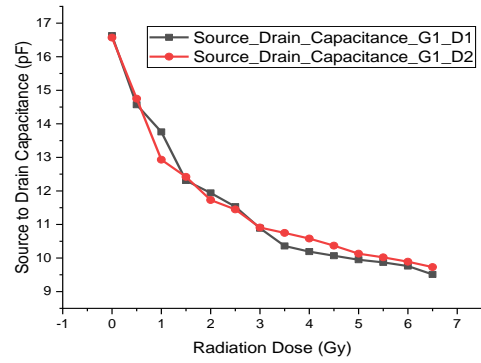


(b)

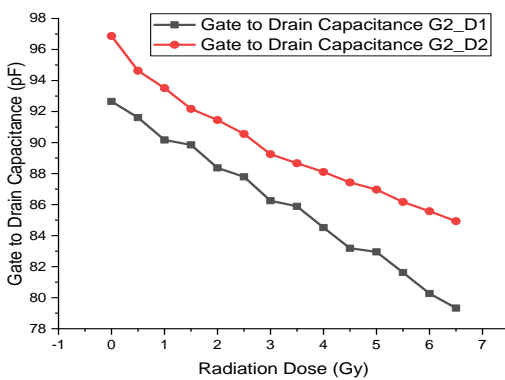
Fig. (9): Represents the n-channel MOSFET gate to source capacitance response to gamma-ray dose; a) first group and b) second group.



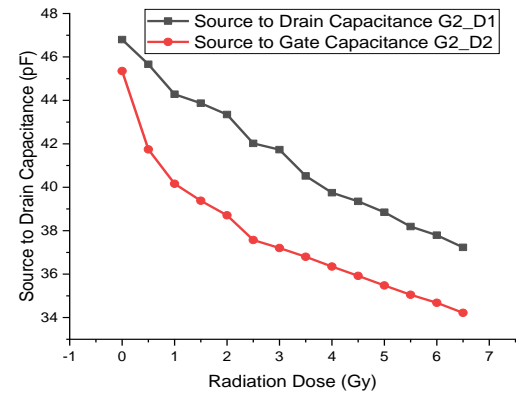
(a)



(a)



(b)



(b)

Fig. (10): Represents the n-channel MOSFET gate to drain capacitance response to gamma-ray dose; a) first group and b) second group.

Fig. (11): Represents the n-channel MOSFET source to drain capacitance response to gamma-ray dose; a) first group and b) second group.

c. Source to Drain Capacitance

The change of source to drain capacitance, C_{sd} , of DUT as a result of ionizing radiation is displayed in Figure 11(a, and b). From Equation (5) and Tables (1, and 3), one can imply that the behavior of C_{sd} is such as obtained from previous discussion. The C_{sd} will be decrement with increasing the dose values. From the schematic diagram in Figure 1, one can notice that C_{sd} is not symbolized. The main reason returned in fact to that the C_{sd} is induced from parallel capacitances summation of C_{sb} , C_{gb} , and C_{db} .

Before we terminate the capacitance section, one can estimate the sensitivity of DUT is starting at unirradiated dose up to 6.5 Gy (the low dose range of study for this work) has linearly decreasing response which implies that it can be used as a dosimeter. Due to fast operation in low gamma doses, fast generation and recombination will be arisen from the oxide and interface traps into device. Moreover, these induced mobile charges will not have the chance to collect into the drain.

To finalize the discussion, some of experimental results are depicted in Figure 12 and 13 before irradiation and at 0.5 Gy for G1 and G2 respectively. Where the relation between I_{ds} and V_{gs} is illustrated and the intercept which determine the threshold is pointed.

The last Figures (14 and 15) indicate the output response pulse after 3 Gy and 0.5 Gy for G1 and G2 respectively. One can recognize that the reference pulse signal considered for comparison studies. In addition, the rise and fall time is displayed which utilized for remainder of determination of previous obtained results. From electronic point of view, analysis of the obtained response pulse signal plays an important role for determining the stability of DUT into an ionizing radiation environment. Not only will contribute for calculating the dynamic performance but also for determining the reliability of this device family to work into space and ionizing radiation applications.

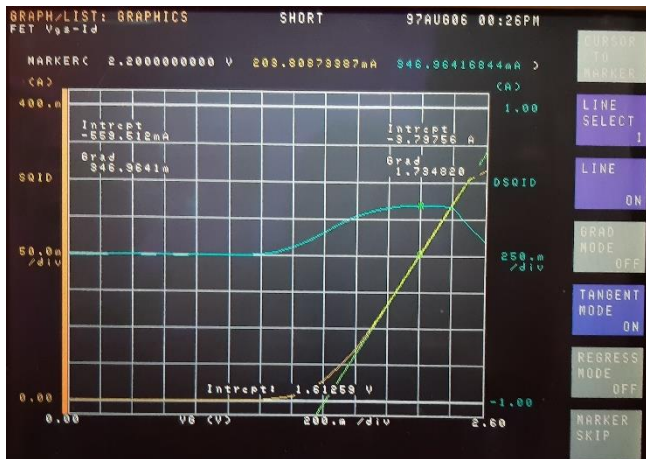


Fig. (12): Sample of measured threshold voltage using HP 4055 semiconductor parameter analyzer first group device one before irradiation.

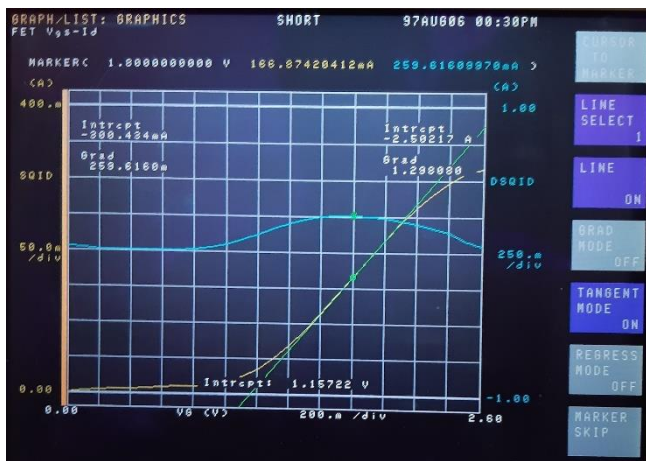


Fig. (13): Sample of measured threshold voltage using HP 4055 semiconductor parameter analyzer second group device two after 0.5 Gy gamma irradiation.



Fig. (14): Sample of measured output pulse (down) with reference input pulse (up) using a digital oscilloscope first group device one after 3.0 Gy gamma irradiation.



Fig. (15): Sample of measured output pulse (down) with reference input pulse (up) using a digital oscilloscope second group device two after 0.5 Gy gamma irradiation.

IV. CONFLICT OF INTEREST STATEMENT

The authors declare that they have no conflict of interest.

V. CONCLUSION

This study presents an experimental work which carried out to determine the N-channel MOSFET dynamic performance under gamma-ray ionizing irradiation. Threshold voltage stability is an essential for any electronic applications. A decrement is happening linearly around the gamma-ray doses of this study from 0.5 to 6.5 Gy. Notified change in dynamic parameters is registered before and after gamma-ray irradiation. In addition, the rise time behaves the same change where it changed linearly with the applied dose. Meanwhile, the fall time was augmented semi-linearly with the gamma-ray dose. The threshold voltage as well as rise and fall times change are very sensitive case for any digital processing because they will be changed the output of the logic gates' status and then gives wrong data. Various capacitances and transconductances between N-channel MOSFET regions are studied. Approximately all values are degraded after exposing to gamma-ray ionizing irradiations. These two later parameters- transconductance and capacitance- were explained and considered numerically and graphically in the result discussion. The main reason of the obtained behavior is returned essentially to the created random mobile charges into the MOSFET channel and oxide layer. Especially into channel oxide region which have different wideness across the device. Exposing recent N-channel MOSFET devices for irradiation will not only benefit for their modern applications but also determines the fidelity of them into hardness work environments. Finally, the family of the investigated devices can also be utilized as a dosimeter in the ionizing radiations facilities and space satellite applications in the considered range.

VI. REFERENCES

- [1] H. M. Mahesh, P. Raghu, C. S. Naveen, K. Mrudula, Shailaja J., Ganesh Sanjeev, Transconductance and Transfer Characteristic of 8 MeV Electron Irradiated Dual N-channel MOSFETs, *Int. J. of emerging tech and advanced engineering*, 4 (9), 247 (2014).
- [2] H. Farroh, A. Nasr, and K. Sharshar, A Study of the Performance of an N-Channel MOSFET under Gamma Radiation as a Dosimeter, *J. of Electronic Materials*, 2020, Springer, Vol. 49, No.10, <https://doi.org/10.1007/s11664-020-08330-4>.
- [3] A. Nasr, Abou El-Maaty M. Aly, A. Sharaf, Study the behaviour of carbon nanotube networks for flow-encoded data, *J. of Electronic Materials*, 2019, Springer, DOI: 10.1007/s11664-019-07526-7.
- [4] Abdelhameed Sharaf, A. Nasr, Ahmed Aboud, Synthesis Characterization and Gamma Irradiation Effect on Cobalt Doped ZnO Diluted Magnetic Semiconductor, *Arab Journal of Nuclear Sciences and Applications*, 55(3), 62 (2022).
- [5] S. Boorboor, S. A. H. Fegghi, H. Jafari, Investigation of Threshold Voltage Shift in Gamma Irradiated N-Channel and P-Channel MOS Transistors of CD4007, *Int. J. of Physical and Mathematical Sciences*, 11(5), 191 (2017).
- [6] Merabtine, N. Benslama, M. Benslama, A. Sadaoui, Dj., Radiation Effects on electronic circuits in a spacial environment, *Semiconductor Physics, Quantum Electronics & Optoelectronics*. 7(4), 395 (2004).
- [7] Bhat, B. R. Sahu, R. P. Radiation Shielding of Electronic Components in INSAT-2. *Journal of Spacecraft Technology*, 3, 36 (1993).
- [8] Srour, J. R. Radiation effects on microelectronics in space. *Proc. IEEE*. 76(11), 1443 (1988).
- [9] Buchman, P., Total Dose Hardness Assurance for Microcircuits for Space Environment. *IEEE Trans. Nucl. Sci.* NS-33(6), 1352 (1986).
- [10] A. Nasr, M. Ashour, Experimental Studies for the Evaluation of Non-Ionizing Radiation Levels”, The Second All African IRPA Regional Radiation Protection Congress, 223 (2007).
- [11] A. Nasr, Effect of ionizing radiation on the characteristics of photodetectors, The Second All African IRPA Regional Radiation Protection Congress, 231(2007).
- [12] Gnana Prakash, A.P. Prashanth, K. C. Ganesh, Nagesha, Y. N. Umakanth, D. Arora, S. K. Siddappa, K. Effect of 30 MeV Li³⁺ ion and 8 MeV electron irradiation on N-channel MOSFETs. *Radiation Effects and Defects in Solids*, 157(3), 323 (2002).
- [13] Sarles, F. W. Stanley, A. G. Roberge, J. K. Godfray, B. M. Space radiation damage measurements in the earth synchronous orbit, *IEEE Trans. Aerosp. Electron. Syst.* 9(6), 921 (1973).
- [14] Jim Schwank, Total Dose Effects in MOS Devices. *IEEE Nuclear Space Radiation Effects Conf., Short Course III-47*, July 2002.
- [15] Benedetto J M and Boesch H E Jr, The relationship between 60Co and 10 KeV x-ray damage in MOS devices, *IEEE Trans. Electron Devices*, 41, 1318 (1986).
- [16] Ma TP, Dressendorfer PV., Ionizing radiation effects in MOS devices and circuits, New York: (John Wiley & Sons; 1989).
- [17] Soubra M, Cygler J, Maskay G. Evaluation of a dual bias metal oxide silicon semiconductor field effect transistors detector as radiation dosimeter. *Med Phys.*, 21(1), 567 (1994).
- [18] Benedetto JM, Boesch HE, McLean FB. Dose energy dependence of interface trap formation in 60Co and X-ray environments. *IEEE Trans Nucl. Sci.*, 35 (6):1260 (1988).
- [19] Oldham TR, McLean FB, Total ionizing dose effect in MOS oxides and devices, *IEEE Trans Nucl Sci.*, 50(6), 483 (2003).
- [20] G. Ristic', S. Golubovic', M. Pejovic, PMOS Transistors for dosimetric Applications, *Electronics Letter*, 29(18), 1644 (1993).
- [21] Goran Ristic', Snežana Golubovic', and Momčilo Pejovic, P-channel metal-oxide-semiconductor dosimeter fading dependencies on gate bias and oxide thickness, *Appl. Phys. Lett.* 66 (1), 88(1995).
- [22] Goran S Ristić, Thermal and UV annealing of irradiated pMOS dosimetric transistors, *J. Phys. D: App. Phys.*, 42, 135101(2009).
- [23] Goran S Ristić, Nikola D Vasović and Aleksandar B Jakšić', The fixed oxide trap modelling during isothermal and isochronal annealing of irradiated RADFETs, *J. of Physics D: Applied Physics*, 45, 305101(2012).

- [24] Nikola D. Vasovic', Goran S. Ristic', A new microcontroller-based RADFET dosimeter reader, *Radiation Measurements*, 47, 272 (2012).
- [25] BaharakEslami, Saleh Ashrafi, Effect of gamma ray absorbed dose on the FET transistor parameter, *J. of Results in physics*, Elsevier, 6, 396 (2016).
- [26] Freeman R, Holmes-Siedle A., A simple model for predicting radiation effects in MOS devices. *IEEE Trans Nucl Sci.*, 25(6), 1216 (1978).
- [27] Pejovic MM, Pejovic MM, Jaksic AB, Contribution of fixed oxide traps to sensitivity of pMOS dosimeters during gamma ray irradiation and annealing at room and elevated temperature, *Sensor Actuator*, 174,85 (2012).
- [28] Holmes-Siedle A, Adams, L., Pauly, B., Marsden, S. Linearity of PMOS radiation dosimeters operated at zero bias, *Electron Lett*, 21, 570 (1985).
- [29] Dasgupta S, Two-dimensional numerical modeling of a deep submicron irradiated MOSFET to extract its global characteristics, *Semicond. Sci. Technol.* 18, 124 (2003).
- [30] M. A. Iqbal, The effect of gamma-ray radiation on n-channel MOSFET, *NSTI-Nanotech*, 1, 104 (2011).
- [31] M.A. Carvajal,, Manuel Vilches, DamiánGuirado, Antonio M. Lallena, J. Banqueri, Alberto J Palma, Readout techniques for linearity and resolution improvement in MOSFET dosimeter, *Sensor Actuator*, A 157, 178 (2010).
- [32] L.J Asensio, M.A. Carvajal, J.A. Lopez-Villanueva, M. Vilches, A.M. Lallena, A.J. Palma, Evaluation of low -cost commercial MOSFET as radiation dosimeter, *Sens. Actuator*, A. 125, 288 (2006).
- [33] M.A.Carvajal, A Mart´nez-Olmos, D P Morales, J A Lopez-Villanueva, A M Lallena, A J Palma, Thermal drift reduction with multiple bias current for MOSFET dosimeters, *Phys. Med. Biol*, 56, 3535 (2011).
- [34] J. Barthe, Electronic dosimeters based on solid state detectors, *Nucl. Inst. Method phys. Res, B*.184, 158 (2001).
- [35] P.H. Halvorsen, Dosimetric evaluation of a new design MOSFET in vivo dosimeter *Med. Phys.* 32, 110 (2005).
- [36] A. Haran, A. Jaksic, N. Refaeli, A. Eliyahu, D. David, J. Barak, Temperature effects and long term fading of implanted and un-implanted gate oxide RADFETs, *IEEE Trans. Nucl. Sci.*, 51 (5), 2917 (2004).
- [37] M. Pejovic, M. Pejovic, B. Jaksic, Radiation sensitive filed effect transistor response to gamma-ray irradiation, *Nucl Technology Radiation protect.* 26(1), 25 (2001).
- [38] S. Mart´nez-García, M.A. Carvajal 1, F.Simancas, J.Banqueri 1, A.M. Lallena, and A.J. Palma, Techniques to increase the sensitivity for dosimeter sensors, *Int. work-conf. on Bioinformatics and Biomedical Eng. (IWBB10)* (2013).
- [39] Sh. M.Eladl, A. Nasr and A. Sharaf, Analysis of a Vertical Cavity Surface Emitting Laser Excited by a Rectangular Pulse, *J. Semiconductor Technology and Science*, 22(1), (2022), <https://doi.org/10.5573/JSTS.2022.22.1.1>.
- [40] ChitikinaNeerajVenkatesh, Guru Prasad Mishra and Biswajit Jena, Design of Core Gate Silicon Nanotube RADFET with Improved Sensitivity, *ECS J. Solid State Sci. Technol.* 11 (08),1002 (2022), <https://doi.org/10.1149/2162-8777/ac8313>.